A theoretical estimation of the pre-breakdown-heating time in the underwater discharge acoustic source

Wang Yi-Bo(王一博)†, Wang Shang-Wu(王尚武), and Zeng Xin-Wu(曾新吾)

College of Opto-electric Science and Engineering, National University of Defense Technology, Changsha 410073, *China*

(Received 4 February 2011; revised manuscript received 31 August 2011)

One of the common characteristics of the electrothermal breakdown in an underwater discharge acoustic source (UDAS) is the existence of a pre-breakdown-heating phase. In our experiment, two phenomena were observed: (1) the breakdown time that takes on high randomicity and obeys a "double-peak" stochastic distribution; (2) the higher salt concentration that reduces the residual voltage and causes 100% non-breakdown. The mechanism of electrothermal breakdown is analysed. To specify the end of the pre-breakdown-heating phase, a "border boiling" assumption is proposed, in which the breakdown time is assumed to be the time needed to heat the border water around the initial arc to 773 K. Based on this 'border boiling' assumption, the numerical simulation is performed to evaluate the effects of two heating mechanisms: the Joule heating from the ionic current, and the radiation heating from the initial arc. The simulation results verify the theoretical explanations to these two experiment phenomena: (1) the stochastic distribution of the radius of the initial arc results in the randomicity of the breakdown time; (2) the difference in efficiency between the radiation heating and the Joule heating determines that, in the case of higher salt concentration, more energy will be consumed in the pre-breakdown-heating phase.

Keywords: pre-breakdown-heating, initial arc, border boiling, residual voltage

PACS: 52.35.Dm **DOI:** 10.1088/1674-1056/21/5/055203

1. Introduction

Discovered by Russian scientist Yutkin, a shock-wave can be generated from underwater discharge, of which the source pressure may reach 10^4 atm. Based on such a mechanical effect, the underwater discharge acoustic source (UDAS) has wide applications in many fields, such as pipe cleaning,[1] rock fragmentation,[2] underwater security,[3] and shockwave lithotrity.[4,5] A typical UDAS is shown in Fig. 1. Its main parts include the energy storage capacitor (C/μF, U_0/ ∼ 10 kV), underwater gap (d/cm) and gas switch.

Due to the weak field strength (∼ 10 kV/cm) in the gap, the breakdown of water in UDAS is usually in the electrothermal mode.[6] The characteristic of the electrothermal breakdown is the existence of the pre-breakdown-heating phase.

Kuzhekin[7] found that in an electric field of 8–36 kV/cm, the breakdown of tap water is delayed by 100–1000 μs. When Olson and Sutton[8] conducted an experimental study on the breakdown of seawater under a 50 kV/cm 233 μs voltage pulse, they concluded that the breakdown delay time is proportional to the threshold energy to evaporate the liquid. Most interesting, Sugiarto *et al.*[9] found experimentally that the suspended leader resulting from the voltage drop on the capacitor, resumes its propagation and completes the breakdown after several hundreds of microseconds. Touya *et al.*[10] found in experiment that under the conditions of $U_0 = 28$ kV, $d = 0.7$ cm, $G_{\text{water}} = 0.02$ S/m, the breakdown time has a strong randomicity, ranging from 40 to 500 μs, and concluded that to realize the breakdown, at least 200 J energy needs to be deposited into the underwater gap.

The randomicity in pre-breakdown-heating time directly causes a great difficulty in realizing a multi-UDAS array. Therefore, the kernel task of this paper is to find a theoretical estimation of the pre-breakdown-heating time. In Section 2 the experiment phenomena are presented and a preliminary analysis of the electro-thermal breakdown is performed. In Section 3 a theoretical model for the properties of the initial arc is proposed. In Section 4 the evolution of the discharge circuit is described. In Section 5 a numerical simulation on pre-breakdown-heating time is carried out. In Section 6 some conclusions are drawn from the present study and the relevant discussion is also made.

†Corresponding author. E-mail: yibowang.nudt@gmail.com

© 2012 Chinese Physical Society and IOP Publishing Ltd

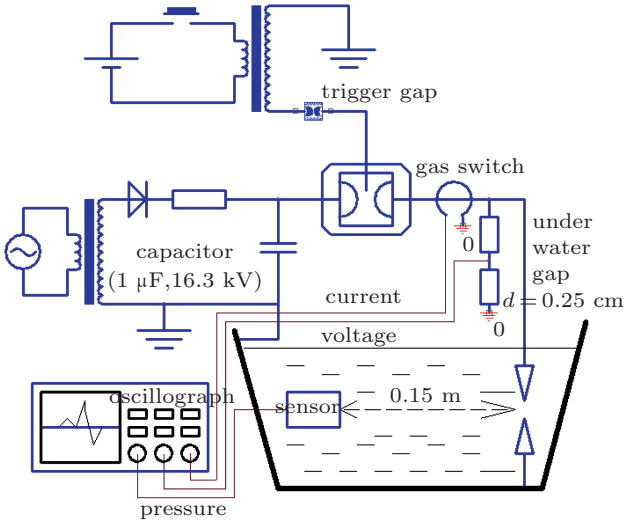


Fig. 1. (colour online) A typical UDAS in our experiment.

2. Analysis to the pre-breakdown-heating process

2.1. Experimental observations on electrothermal breakdown

As shown in Fig. 1, in our measuring system, the sample resistors and the Rokovski coil produce the signals of the gap voltage and the discharge current respectively. The pressure sensor is placed at a point 15 cm away from the underwater gap. The oscillograph records the voltage, current, and pressure signals synchronously at a rate of 10 MHz.

A small capacitor (1 μF), a fixed low voltage (16.3 kV) and a fixed gap spacing (0.25 cm) are used in the experiment. This initial energy is around the breakdown threshold. Under these initial conditions, both the breakdown and the non-breakdown may occur.

Under the above fixed initial conditions, the influences of three different salt concentrations (G = 0.037 S/m, 0.28 S/m, 3 S/m) on breakdown are tested experimentally. Because of the high randomicity in electrothermal breakdown, the discharge is repeated over 100 times for each salt concentration. The most important evolution curves of the gap voltage are shown in Figs. 2–4. In each figure, the average breakdown time, the average residual voltage at the breakdown moment and the non-breakdown probability are summarized.

According to Figs. 2–4, the conductivity of water has two kinds of influences on electro-thermal breakdown:

(1) higher conductivity leads to shorter average breakdown time;

(2) higher conductivity leads to lower average residual voltage.

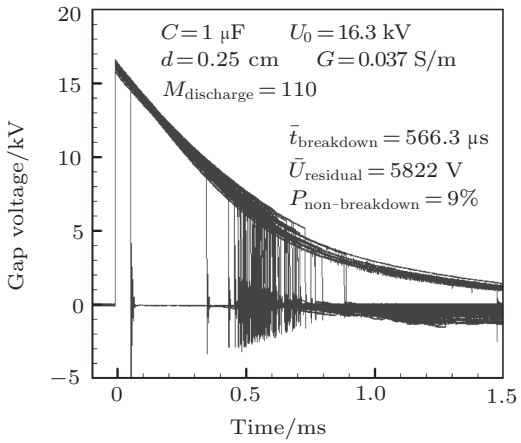


Fig. 2. Voltage evolution under G = 0.037 S/m, with $M_{\text{discharge}}$ being the repetition number of the discharge, $\bar{t}_{\text{breakdown}}$ the average breakdown time, $\bar{U}_{\text{residual}}$ the average residual voltage, and $P_{\text{non-breakdown}}$ the non-breakdown probability.

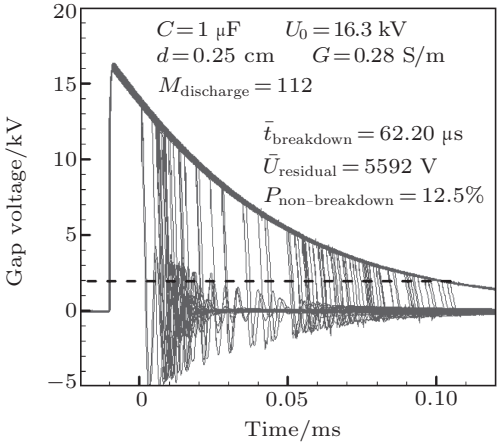


Fig. 3. Voltage evolution under G = 0.28 S/m.

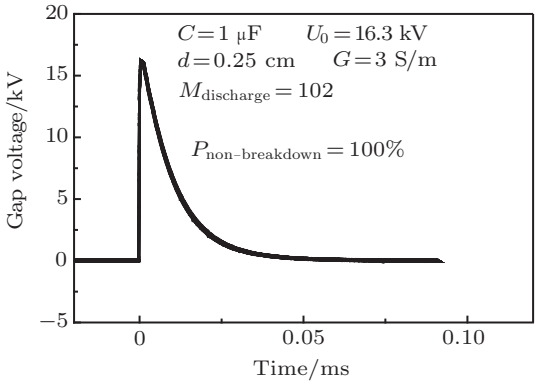


Fig. 4. Voltage evolution under G = 3 S/m.

The first effect reveals that ionic current plays an important role in electrothermal breakdown. The

mechanism of the second effect is more complicated and it will be discussed in Secitons 3 and 4.

In addition, in order to obtain an intuition about the distribution of the breakdown time, the time axis is divided into $(t_1 \ldots t_n \ldots t_N)$ at intervals of 1 μs. Meanwhile, the breakdown moments in the 110 groups of voltage data are marked by $(t_{b1} \ldots t_{bm} \ldots t_{bM}, M > 100)$. The contribution of the m-th breakdown time to the n-th time point is assumed to

$$P_{m\to n} = \exp\left[-\frac{(t_{bm} - t_n)}{\sigma^2}\right]. \quad (1)$$

The total distribution weight can be described as

$$P_n = \sum_{m=1}^{M} P_{m\to n}. \quad (2)$$

For $G = 0.037$ S/m, we choose $\sigma = 20$ μs, and for $G = 0.28$ S/m, we choose $\sigma = 4$ μs. Under these rules, the distribution weight of the breakdown time is shown in Figs. 5 and 6.

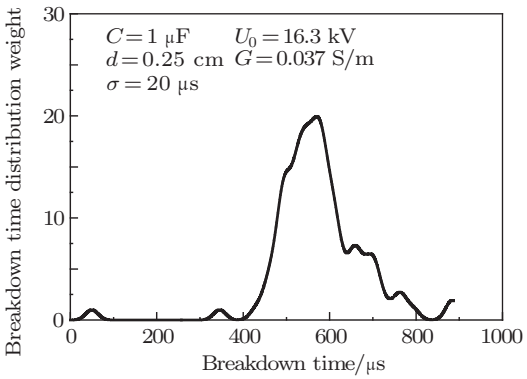


Fig. 5. Distribution weight of breakdown time under $G = 0.037$ S/m.

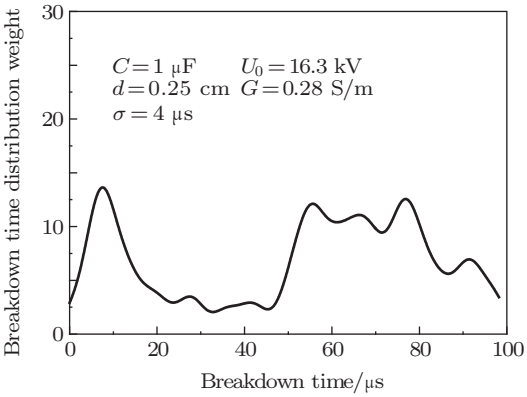


Fig. 6. Distribution weight of breakdown time under $G = 0.28$ S/m.

As shown in Figs. 5 and 6, the breakdown time obeys a "double-peak" distribution in the main. In water of higher conductivity ($G = 0.28$ S/m), probability of the "fast" breakdown is higher.

To understand the characteristics of this special breakdown mode, we must make a preliminary analysis of the initial phase of the underwater breakdown.

2.2. Initial phase of electrothermal breakdown

Different from the breakdown in gas, compactly distributed water molecules set a high threshold of field strength for direct breakdown, which is usually several MV/cm. However, the bonding between liquid molecules is not so strong as that between solid molecules. The heating and the evaporation of water increase the interval between the molecules and then reduce that threshold. According to Fig. 3, even if the average field strength drops to 8 kV/cm (2 kV/0.25 cm), breakdown still happens. Therefore, we can infer that the heating and the evaporation of water is necessary for electrothermal breakdown.

When a voltage pulse is applied to the underwater gap, the local amplified electric field on the surface of the electrodes field will form many "ignition" areas filled with hot plasma. The kinetic expansion of these "ignition" areas will generate a weak shockwave (called "ignition shockwave" in this paper). In water of high salt concentration, the ignition shockwave is detectable. As shown in Fig. 4, under $G = 3$ S/m, $d = 0.25$ cm, non-breakdown happens 100%. When the gap interval is reduced to 0.2 cm, both breakdown and non-breakdown may occur. The evolution curves of gap voltage and shockwave pressure are shown in Fig. 7.

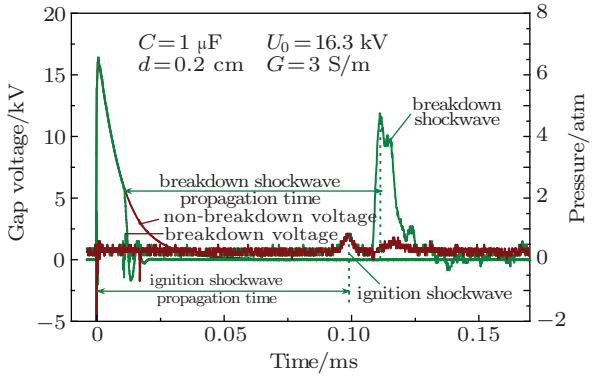


Fig. 7. (colour online) Gap voltage and shockwave pressure under $G = 3$ S/m, $d = 0.2$ cm.

As shown in Fig. 7, in an environment of high conductivity ($G = 3$ S/m), every discharge, no matter if it is breakdown or non-breakdown, generates nearly

the same ignition shockwave. The breakdown shockwave arrives at a random delayed time, which can be regarded as the breakdown time.

The succeeding development of ignition areas is the key to breakdown. In the dynamic breakdown, which has been long studied by Jones and Kunhardt,[11] Martin *et al.*,[12] Korobeynikov,[13] and others, the applied field strength reaches several 100 kV/cm. In such an electric field, the electrons in ignition areas provide enough heating power to quickly evaporate the border water around the ignition area. Therefore, the evaporation and the ionization cycles are capable of proceeding continuously, which forms many leader channels and finally leads to breakdown.

Under the working conditions of a UDAS, there is no strong electric field between the electrodes, and the heating of the border water around the ignition areas is not sufficient to generate a leader channel immediately when the voltage is applied to the gap. However, the propagation of the leader channel does not suspend completely at this moment. The discharge plasma in the ignition area will extend to the opposite electrode under the electrostriction force until it bridges the underwater gap. That process is called "streamer connection" in this paper.

Streamer connection does not necessarily cause a breakdown.[6] The term "streamer" used in this paper is interpreted as "slow streamer" by Kukhta and Lopatin.[14] Different from the leader channel ("fast streamer"),[14] the streamer is in fact the extension of the ignition area rather than the ionization of gap water. The final product of the streamer connection, the "initial arc", can be seen as a gas bridge.[6] Therefore, the initial arc will neither evidently expand nor lead to breakdown.

Though the initial arc does not cause breakdown, the discharge plasma inside it provides a radiation heating power for the border water around it. Touya *et al.*[10] observed a stable ultra-violet (UV) radiation in pre-breakdown phase.

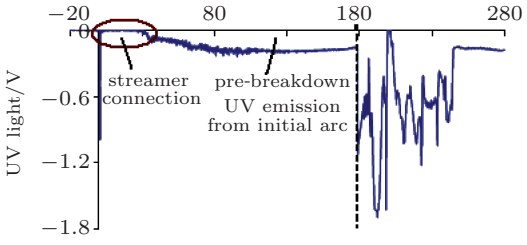


Fig. 8. (colour online) Pre-breakdown UV emission observed by Touya *et al.*[10]

The role of the initial arc in the pre-breakdown-heating process will be analysed below.

2.3. Analysis of the pre-breakdown-heating process

According to the above analysis, electrothermal breakdown can be described as four phases:

After the ignition/streamer connection phase, the radiation heating from the initial arc together with the Joule heating from the ionic current, provides a "slow" heating for the border water, as shown in Fig. 10.

If the temperature of the border water reaches a threshold value, the thermal kinetic energy of the water molecules will be enough to overcome the hydrogen bond between them. When the water molecules can easily enter the initial arc, the evaporation-ionization cycle will develop continuously. Here the term "border boiling" is used to describe the end of the pre-breakdown-heating process.

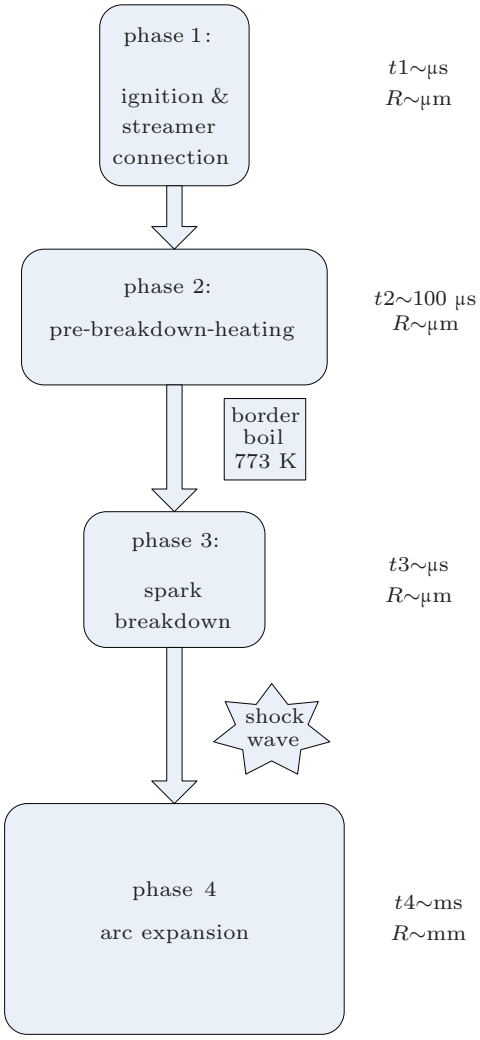


Fig. 9. Four phases in electrothermal breakdown.

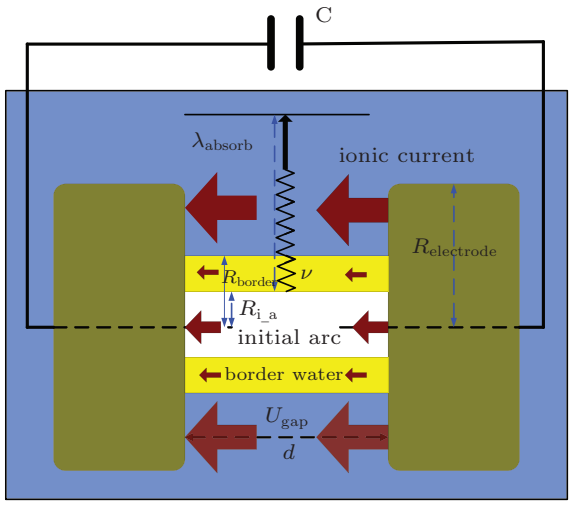


Fig. 10. (colour online) Pre-breakdown-heating on border water, with R_{border} being the radius of the border water (as an equivalent cylinder), R_{i_a} the radius of the initial arc, $R_{electrode}$ the radius of the cross section of the electrode (as an equivalent cylinder), and λ_{absorb} the characteristic absorption scope of the radiation in water.

The threshold temperature for border boiling is set to be 773 K. That assumption is inferred from the thermal capacity of water (4.2 J/gK) and the gasification energy of water (2000 J/g).

The non-breakdown events recorded in Figs. 2 and 3 reveal that the "border boiling" is not the unique necessary condition for electrothermal breakdown. Another necessary condition is that when "border boiling" is realized, there will be a strong enough field in the gap. According to Fig. 3, the threshold field strength is about 8 kV/cm (2 kV/0.25 cm), which coincides with the necessary field strength observed by Kuzhekin (8–36 kV/cm).[7] That threshold field strength means that enough residual voltage on the capacitor is required at the "border boiling" moment. So, a coupled model, which covers both the pre-breakdown-heating process and the evolution of the discharge circuit, is needed.

As shown in Fig. 9, the temperature of the border water can be described by an equation of energy equilibrium as

$$C_{water} \cdot (\rho S_{border} d) \cdot (T_{border} - T_{water_0}) \approx \int_0^t U_{gap}^2(t) G_{water} \frac{S_{border}}{d} \mathrm{d}t + \int_0^t \left[P_{border}^{i_a}\right] \mathrm{d}t, \quad (3)$$

where C_{water} is the thermal capacity of water, $\rho S_{border} d$ the equivalent mass of the border water, T_{border} the temperature of the border water, T_{water_0} the initial temperature of the water, $U_{gap}(t)$ the voltage across the underwater gap, G_{water} the conductivity of water, and $P_{border}^{i_a}$ the radiation heating power from the initial arc. Equation (3) is developed to solve two issues:

a) border boiling time t_{boil}, which is defined as the time to raise the border temperature T_{water_0} to border boiling temperature T_{boil}. t_{boil} can be taken as a measure of the breakdown time $t_{breakdown}$.

b) The residual voltage $U_{residual}$, which is defined as the voltage on the capacitor at the border boiling moment.

Prior to the solving of Eq. (3), the radiation heating power $P_{border}^{i_a}$ and the gap voltage $U_{gap}(t)$ should be obtained.

3. Radiation heating power from the initial arc

After streamer connection (phase 1 in Fig. 9), the initial arc usually exists stably for several hundreds of microseconds without evident expansion, which means that the pressure of the initial arc does not deviate much from the static pressure (usually 1 atm). The pre-breakdown UV light emission observed by Touya *et al.*[10] means that the temperature of the initial arc is high. According to $p \approx nkT$, the density of the initial arc must be much lower than that at room temperature gas. At such a high temperature and low-density status, the discharge plasma in the initial arc will be fully ionized.

The stable status of the initial arc also means that the energy injection power P^+ and the energy dissipation power P^- are balanced, i.e.,

$$P^+(T) \approx P^-(T), \quad (4)$$

where P^+ is the energy injection power that is provided by the discharge circuit, and it is proportional to the cross-sectional area of the initial arc and related to the conductivity (σ_{i_a}) of the initial arc by

$$P_E^+ = \frac{U_{gap}^2}{Z_{i_a}} = U_{gap}^2 \cdot \sigma_{i_a}(T) \cdot \frac{\pi R_{i_a}^2}{d}. \quad (5)$$

Here R_{i_a} can be regarded as the average radius of the initial arc, and σ_{i_a} is the conductivity of the full y ionized discharge plasma in the initial arc.

According to Golant *et al.*[15] the conductivity of fully ionized plasma is related to temperature by

$$\sigma = \frac{n_e e^2}{m_e \upsilon_{ei}}, \quad (6)$$

$$\upsilon_{ei} = \frac{4\sqrt{2}\pi}{3} \frac{n_e K^2 e^4}{m_e^{1/2} (kT)^{3/2}} L_e \quad (K = \frac{1}{4\pi\varepsilon_0}), \quad (7)$$

$$L_{\rm e} = \ln\left[\frac{(kT)^{3/2}}{e^3K^{3/2}n^{1/2}}\right] = \ln\left[\frac{(kT)^2}{K^{3/2}e^3\,(0.5P_0)^{1/2}}\right]. \quad (8)$$

To simplify these formulae, we adopt a unit system for the relevant physical quantities as below:
1) temperature: $T = \tilde{T}\cdot[10^4\ \mathrm{K}]$,
2) voltage: $U = \tilde{U}\cdot[10^4\ \mathrm{V}]$,
3) capacitor: $C = \tilde{C}\cdot[\mu\mathrm{F}]$,
4) macroscopical dimension: $d = \tilde{d}\cdot[\mathrm{cm}]$,
5) microcosmic dimension: $R_{\rm i_a} = \tilde{R}_{\rm i_a}\cdot[\mu\mathrm{m}]$,
6) pressure: $P = \tilde{P}\cdot[\mathrm{atm}]$,
7) the remaining variables: SI unit.

Under the rules for units, $L_{\rm e}$ and $\sigma_{\rm i_a}$ are simplified as

$$L_{\rm e} = 3.2 + 2\ln\tilde{T} - \frac{1}{2}\ln\tilde{P}_0, \quad (9)$$

$$\sigma_{\rm i_a} = \tilde{\sigma}_{\rm i_a}\left[\frac{S}{m}\right] = \left[\frac{8133}{(3.2+2\ln\tilde{T})}\left(\tilde{T}\right)^{3/2}\right]\left[\frac{S}{m}\right]. \quad (10)$$

When the stable discharge plasma is generated in the initial arc, the temperature will reach 10^4 K order. Then, the main energy dissipation mechanism is the electromagnetic radiation, which holds back the temperature of the discharge plasma from further increasing. The rate of radiation loss can be estimated by the black-body radiation principle:

$$P^- \approx sT^4 2\pi d R_{\rm i_a} \quad (s = 5.67\times10^{-8}\ \mathrm{W/m^2\cdot K^4}). \quad (11)$$

According to Eqs. (5)–(11), equation (4) can be simplified into a dimensionless form:

$$6.868\frac{\tilde{U}_{\rm gap}^2\tilde{R}_{\rm i_a}}{\tilde{d}^2} = [3.2+2\ln\tilde{T}]\tilde{T}^{5/2}. \quad (12)$$

Assuming $L_{\rm e}$ to be constant $L_{\rm e} = [3.2+2\ln\tilde{T}] \approx 6.868$ leads to

$$\tilde{\sigma}_{\rm i_a} \approx 1184.2\left(\tilde{T}\right)^{3/2}, \quad (13)$$

$$\tilde{T} \approx \left[\frac{\tilde{U}_{\rm gap}^2(t)\tilde{R}_{\rm i_a}}{\tilde{d}^2}\right]^{0.4}, \quad (14)$$

During the pre-breakdown-heating phase (phase 2 in Fig. 9), the voltage on the capacitor decreases continuously. As a result, the initial arc usually experiences a radial shrink. If the particle number and the pressure of the initial arc keep constant, from $p \approx nkT$ we can estimate the radius of the initial arc at any time in the pre-breakdown-heating phase:

$$R_{\rm i_a} = R_{\rm i_a_0}T^{1/2}/T_0^{1/2}. \quad (15)$$

Here, $R_{\rm i_a_0}$ is the radius when the initial arc reaches a stable state immediately after the streamer connection. Eqs. (14) and (15) can be further simplified into

$$\tilde{T} = \frac{\tilde{U}_{\rm gap}}{\tilde{d}}\sqrt{\frac{\tilde{R}_{\rm i_a_0}}{\tilde{T}_0^{1/2}}}, \quad (16)$$

$$\tilde{R}_{\rm i_a} = \sqrt{\frac{\tilde{U}_{\rm gap}}{\tilde{d}}\frac{\tilde{R}_{\rm i_a_0}^{5/2}}{\tilde{T}_0^{5/4}}}. \quad (17)$$

From Eqs. (11)–(17), the total radiation power from the initial arc can be estimated. Cook *et al.*[16] thought that the infrared (IR) radiation from the initial arc, which took up about 30% of the total radiation power, was the main heating source for the border water. To simplify the problem, we assume that the power of IR radiation takes up an ω portion of the whole radiation power, the characteristic decay distance is $\lambda_{\rm absorb}$, and the radius of the border water is $R_{\rm border}$. The IR radiation power which deposits in the shell $[R_{\rm i_a},\ R_{\rm border}]$ can be estimated by

$$P_{\rm border}^{\rm i_a} = P_\nu^-\omega\left[1-\exp\left(-\frac{R_{\rm border}-R_{\rm i_a}}{\lambda_{\rm absorb}}\right)\right] \approx U_{\rm gap}^2\sigma_{\rm i_a}\frac{\pi R_{\rm i_a}^2}{d}\omega\frac{R_{\rm border}-R_{\rm i_a}}{\lambda_{\rm absorb}}. \quad (18)$$

According to Eqs. (13), (14), and (15), $P_{\rm border}^{\rm i_a}$can be expressed by $U_{\rm gap}(t)$ which will be solved in Section 4. Eliminating the cross-sectional area $S_{\rm Border} = \pi(R_{\rm border}^2 - R_{\rm i_a}^2)$ of border water, Eq. (3) can be reduced to a dimensionless form as

$$(\tilde{T}_{\rm border} - \tilde{T}_{\rm water_0}) = 23.8\Big\{\int_0^t\frac{\tilde{U}_{\rm gap}^2(t)\tilde{G}_{\rm water}}{\tilde{d}^2}\,{\rm d}t + \int_0^t\left[\frac{\tilde{U}_{\rm gap}^4(t)}{\tilde{d}^4}\cdot\frac{1184.2\tilde{R}_{\rm i_a_0}^2}{10^4\tilde{\lambda}_{\rm absorb}\tilde{T}_{\rm i_a_0}} \times\frac{\omega}{R_{\rm border}/R_{\rm i_a}+1}\right]{\rm d}t\Big\}. \quad (19)$$

We assume that about 30% of the radiation power from the initial arc is absorbed by the border water; the characteristic decay distance of the IR light is 1 cm and the scope of the border water is $R_{\rm border} = 2R_{\rm i_a}$, the constants in Eq. (19) can be defined as

$$\tilde{\lambda}_{\rm absorb} = 1, \quad (20)$$

$$\frac{\omega}{R_{\rm border}/R_{\rm i_a}+1} \approx 0.1. \quad (21)$$

The threshold temperature for border boiling, $T_{\rm boil}$, is assumed to be

$$\tilde{T}_{\rm boil} \hat{=} 0.0773. \quad (22)$$

In Eq. (19), the ratio of the radiation heating power to the Joule heating power, in fact describes the efficiency of the pre-breakdown-heating process

$$\beta \hat{=} \frac{\tilde{U}_0^2}{2\tilde{G}_{\rm water}\tilde{d}^2} \times \left[\frac{\tilde{R}^2_{\rm i_a_0}}{\tilde{\lambda}_{\rm absorb}\tilde{T}_{\rm i_a_0}} \cdot \frac{0.1184\omega}{R_{\rm border}/R_{\rm i_a}+1}\right]. \quad (23)$$

Breakdown always happens in the border layer around the initial arc. The radiation heating from the initial arc is an efficient local heating mechanism, while the Joule heating from the ionic current is an inefficient heating mechanism. We can infer from Eq. (23) that in the case of higher salt concentration, more energy will be consumed in the pre-breakdown-heating process. This conclusion can explain the results in Figs. 3 and 4 that when the salt is added into the water, the average residual voltage decreases and so non-breakdown may happen 100%.

As discussed in Section 2, the initial arc is the kinetic extension of the ignition area from one electrode to another. Just like the streamer process in air, the shape and the position of the initial arc take on evident randomicity. We can infer from Eq. (19) that the randomicity in the initial arc finally results in the randomicity in breakdown time.

In addition, as shown in Fig. 6, when a little salt is added into water ($G = 0.28$ S/m), the distribution of breakdown time becomes an evident "double-peak" structure. That means that in the case of higher conductivity, another kind of initial arc is generated. It may be the kinetic extension of the cathode ignition area and it is called the "cathode initial arc" in this paper. Different from the case of the anode initial arc, the average radius of the cathode initial arc is bigger.[6] However, the occurrence of the cathode initial arc needs higher voltage or higher conductivity.[6]

In the numerical simulation in Section 5, the radius of initial arc will be assumed to obey a "double-peak" normal distribution.

The stochastic distribution shown in Fig. 11 can be described as

$$f(R_{\rm ia}) = \frac{1}{(1+\theta_{\rm c_ia})} \frac{\exp\left[-\dfrac{(R_{\rm ia}-R_{\rm av_a_ia})^2}{2\sigma^2_{\rm sd_a_ia}}\right]}{\sqrt{2\pi}\sigma_{\rm sd_a_ia}} + \frac{\theta_{\rm c_ia}}{(1+\theta_{\rm c_ia})} \frac{\exp\left[-\dfrac{(R_{\rm ia}-R_{\rm av_c_ia})^2}{2\sigma^2_{\rm sd_c_ia}}\right]}{\sqrt{2\pi}\sigma_{\rm sd_c_ia}}. \quad (24)$$

Here, the meanings of $R_{\rm av_a_ia}$, $\sigma_{\rm sd_a_ia}$, $R_{\rm av_c_ia}$, $\sigma_{\rm sd_c_ia}$ are already shown in Fig. 11. The $\theta_{\rm c_ia}$ is the ratio of the cathode initial arc to the anode initial arc. In the case of higher salt concentration, $\theta_{\rm c_ia}$ is higher. The effect of the "double-peak" distribution of probability will be shown with the simulation results in Section 5.

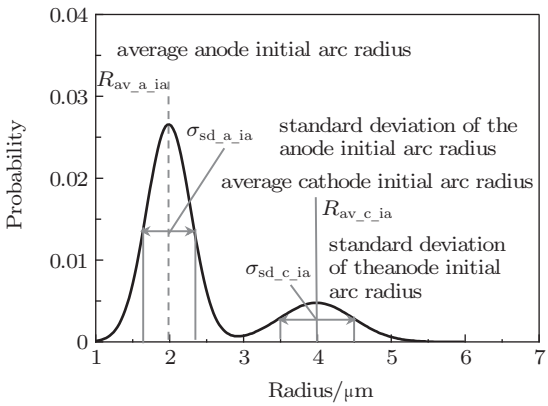


Fig. 11. The "double peak" normal distribution of probability.

4. Voltage on the gap in the pre-breakdown-heating phase

As described in Section 2, the aim of pre-breakdown-heating is to heat the border water to the "border boiling" temperature. Therefore, voltage on the capacitor usually undergoes an evident decrease. Besides our experimental results shown in Figs. 2 and 3, Touya *et al.*[10] measured voltage on the gap also verified that effect as shown in Fig. 12.

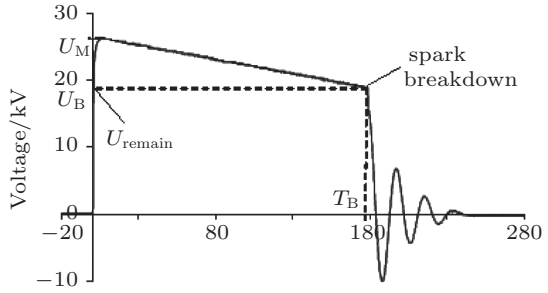


Fig. 12. Pre-breakdown voltage-leakage observed by Touya *et al.*[10]

Because $U_{\rm B}$ in Fig. 12 usually refers to the breakdown strength, we substitute $U_{\rm B}$ of Ref. [10] with $U_{\rm residual}$ in this paper.

In the pre-breakdown-heating phase, the resistance of the underwater gap is far bigger than that in the outer discharge circuit. $U_{\rm gap}(t)$ can be estimated by the voltage on the capacitor as

$$U^2_{\rm gap}(t) \approx U_0^2 \exp\left[-\frac{t}{CZ_{\rm gap}}\right]. \quad (25)$$

Here, $Z_{\rm gap}$ is the equivalent resistance of the underwater gap and it can be estimated by

$$Z_{\rm gap} = \frac{d}{G_{\rm water}\pi R'^2_{\rm electrode}}. \quad (26)$$

Here, $R'_{\rm electrode}$ is the equivalent radius of the water cylinder between two electrodes. A simple estimation by "$R'_{\rm electrode} = R_{\rm electrode} = D_{\rm electrode}/2$" usually leads to a totally wrong result in the numerical simulation. Because of the complicated structure of electrodes, $R'_{\rm electrode}$ is bigger than $D_{\rm electrode}/2$ and it is difficult to estimate $Z_{\rm gap}$ theoretically. Instead, in our simulation, $Z_{\rm gap}$ is estimated by the gap evolution curve in a non-breakdown event as shown in Fig. 13.

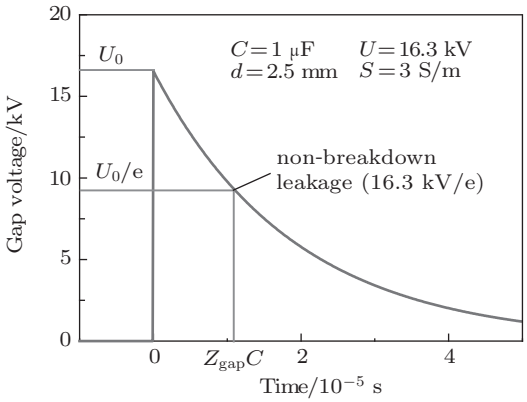


Fig. 13. Estimation of $Z_{\rm gap}$ by experimental result.

When $Z_{\rm gap}$ is estimated, $R'_{\rm electrode}$ can be estimated from $G_{\rm water}$ and d, which can be regarded as a constant for different values of water conductivity $G_{\rm water}$ under fixed gap interval d. For the electrodes used in our experiment, when $G = 3$ S/m, we obtain $Z_{\rm gap} \approx 12\ \Omega$ and $R'_{\rm electrode} \approx 0.47$ cm.

The ratio of the evaporation energy of the equivalent water cylinder to the initial energy is defined as

$$\gamma = \frac{C_{\rm water}\rho(\pi R'^2_{\rm electrode}d)(T_{\rm boil} - T_{\rm water_0})}{0.5CU_0^2}. \quad (27)$$

Based on β in Eq. (23) and γ in Eq. (27), if the analytical approximation (25) is used for $U_{\rm gap}$, the $t_{\rm boil}$ and $U_{\rm remain}$ can be estimated as

$$U^2_{\rm remain} \approx U_0^2\left[\frac{\sqrt{4\beta(\beta+1-\gamma)+1}-1}{2\beta}\right], \quad (28)$$

$$t_{\rm boil} \approx \left[-\frac{C}{Z_{\rm gap}}\right]\ln\left[\frac{U_{\rm remain}}{U_0}\right]. \quad (29)$$

The condition for border boiling can be deduced from expression (28) as

$$\beta + 1 > \gamma. \quad (30)$$

Criterion (30) shows that the electrothermal breakdown sets a definite requirement for the energy stored in the capacitor, and the higher the conductivity, the higher the requirement for the initial energy is. In our experiment on tap water (Fig. 2) $G = 0.037$ S/m, $C = 1\ \mu$F, $U_0 = 16.3$ kV, $d = 0.25$ cm, and $R'_{\rm electrode} \approx 0.47$ cm, from Eqs. (23) and (27), we can have $\beta = 1.52\tilde{R}^{1.6}_{\rm i_a_0}$, and $\gamma = 2.62$. That means that the realization of border boiling in tap water is possible when $R_{\rm i_a_0} > 1.1$ μm. In sea water, $G = 3$ S/m, $\beta \ll 1$, and $\gamma = 2.62$. That means that the initial energy in the capacitor is not enough to realize border boiling, which gives an explanation for the 100% non-breakdown recorded in Fig. 4.

The above analysis verifies the conclusion in Section 3 that the radiation heating from the initial arc is an efficient local heating mechanism, while the Joule heating from the ionic current is an inefficient heating mechanism. Here we can infer that to realize border boiling in seawater, the energy stored in the capacitor must exceed the energy for evaporating the equivalent water cylinder between two electrodes.

5. Simulation on the pre-breakdown-heating process

According to the analysis in Sections 2, 3, and 4, the simulation routine for the discharge process can be described as

In Fig. 14, $E_{\rm spark}$ is the threshold field strength for breakdown. According to our experimental result and Kuzhekin's result,[7] $E_{\rm spark} \approx 8$ kV/cm.

After breakdown, the border water is converted into an evident arc. Then, $Z_{\rm gap}$ can be estimated from Eq. (13) as

$$Z_{\rm breakdown} \approx 2.69 \times 10^6 \frac{\tilde{d}^{2.2}}{\tilde{U}^{1.2}_{\rm remain}\tilde{R}^{2.6}_{\rm arc}} \quad [\Omega]. \quad (31)$$

In the simulation, $R_{\rm arc} = 50$–100 μm. The accurate estimation of $Z_{\rm breakdown}$ needs a more complicated computation on the arc expansion process, and this is not going to be done here. After breakdown, the inductance (L) of the discharge circuit may not be ignored. Then, the discharge circuit can be simulated by

$$I_{n+1} \approx \frac{U_n\Delta t - I_n(\Delta t)^2/2C + LI_n}{[Z_{\rm ex} + Z_{\rm breakdown}]\Delta t + L + \Delta t^2/2C}, \quad (32)$$

$$U_{n+1} \approx U_n - \frac{1}{2C}(I_{n+1} + I_n)\Delta t. \quad (33)$$

For the initiation of the numerical simulation, besides the common parameters such as capacitor C, charging voltage U, water conductivity G, water temperature $T_{\text{water_0}}$, gap interval d, and electrode diameter D, the most important parameters are the non-breakdown leakage resistance Z_{gap} and the stochastic properties of the initial arc.

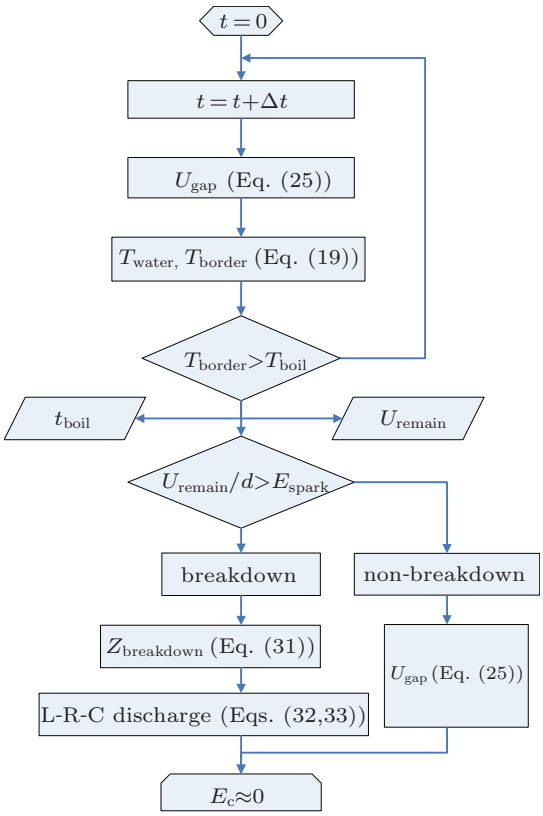


Fig. 14. Simulation routine for discharge.

To obtain the Z_{gap}, only a simple experiment is needed, from which the equivalent radius of the water cylinder between the electrodes ($R'_{\text{electrode}}$) can be estimated.

For each salt concentration (G = 0.037 S/m, 0.28 S/m, 3 S/m), the evolution of the gap voltage is simulated 100 times. In every individual simulation, the radius of the initial arc is sampled from the "double-peak" normal distribution as shown in Fig. 11. The stochastic properties of the initial arc, $R_{\text{av_a_ia}}$, $\sigma_{\text{sd_a_ia}}$, $R_{\text{av_c_ia}}$, $\sigma_{\text{sd_c_ia}}$, $\theta_{\text{c_ia}}$ are defined in a tentative way.

Under the fixed conditions: C = 1 μF, U = 16.3 kV, d = 0.25 cm, $D_{\text{electrode}}$ = 0.4 cm, the simulation results of the gap voltage for different salt concentrations are shown in Figs. 15–17. To compare with the experimental results, the average simulation breakdown time, the average simulation residual voltage, the non-breakdown probability and the experimental non-breakdown curve are added to the plots. For the 100% non-breakdown event, the maximum radius of the initial arc is tested.

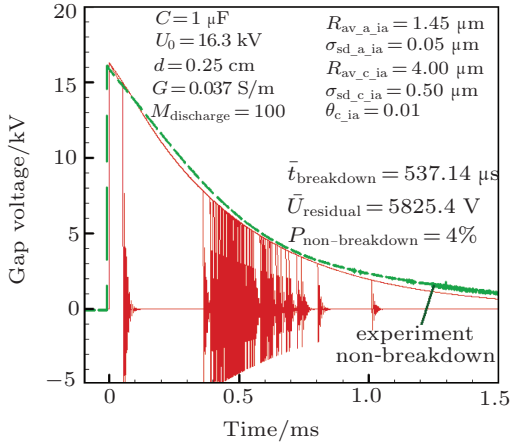


Fig. 15. (colour online) Simulation result of gap voltage, with G = 0.037 S/m.

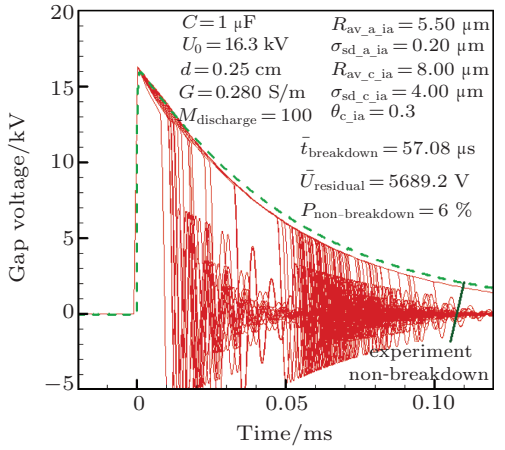


Fig. 16. (colour online) Simulation result of gap voltage, with G = 0.28 S/m.

From the simulation results shown in Figs. 15–17, we can draw the following conclusions.

1) The variation range of the simulated breakdown time in tap water (50–1000 μs) does not deviate much from either our experimental results (50–900 μs) or Kuzhekin's[7] (100–1000 μs). The "double-peak" normal distribution of the radius of the initial arc leads to a separation of "fast" breakdown from "slow" breakdown.

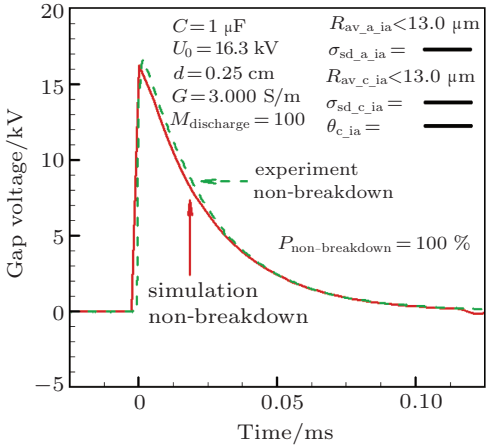


Fig. 17. (colour online) Simulation result of gap voltage, with $G = 3$ S/m.

2) The simulated residual voltages under different salt concentrations (see Figs. 15 and 16) coincide with the corresponding experimental results (see Figs. 2 and 3), thereby verifying the analytical explanation that the pre-breakdown-heating process in salty water consumes more energy;

3) The simulation results verify the assumption of the border boiling temperature. Under this basic assumption of 773 K (500 °C), the simulation results are in good agreement with the experimental data.

6. Conclusion and discussion

In this paper, two necessary conditions of electrothermal breakdown are concluded for the "realization of the border boiling around the initial arc" and "enough residual voltage at the border boiling moment". The heating effects from the initial arc and the ionic current are simulated. The simulation results reveal that the initial arc acting as the "seed" of the breakdown plays a key role in the high randomicity of breakdown time. Therefore, a further study of the ignition/streamer connection phase is needed. A possible method to overcome the randomicity of breakdown time as reported by Lu *et al.*[17] is to use a thin metal wire (20 μm) rather than the initial arc as the breakdown seed.

The present model for the pre-breakdown heating process is in fact a zero-dimensional and semi-empirical model. Many critical variables, such as electric field strength E and radius of the initial arc are analysed and simulated only in their average value. A full 2D model, which should take into account more physical and chemical process, is necessary for the accurate prediction of the behaviour of a UDAS. Especially, an accurate optical observation on the ignition/streamer connection process (phase 1 in Fig. 9), which evidently influences the structure and the position of the initial arc, is needed.

References

[1] Hofman J and Weisse H 1997 11*th IEEE Pulsed Power Conf.* (Baltimore: MD) p. 203

[2] Hamelin M, Kitzinger F, Pronko S and Schofield G 1993 *Proceedings of the 9th IEEE Pulsed Power Conference*, (Albuquerque: NM) p. 11

[3] Winsor N 1997 *Technology Report for United States Navy and Marine Corps* 2000

[4] Coleman A, Saunders J, Preston R and Bacon D 1987 *Ultrason. Med. Biol.* **13** 651

[5] Delius M, Jordan M, Eizenhoefer H, Marlinghaus E, Heine G, Liebich H and Brendel W 1989 *Ultrason. Med. Biol*, **14** 689

[6] Vasily Y Ushakov 2007 *Impulse Breakdown of Liquids*, (Berline: Springer) pp. 172, 357

[7] Kuzhekin I P 1966 *Zh. Tekh. Fiz.* **36** 2125

[8] Olson A H and Sutton S P 1993 *J. Acoust Soc. Am.* **94** 2226

[9] Sugiarto A T, Sato M and Skalny J D 2001 *J. Phys.* D: *Appl. Phys.* **34** 3400

[10] Touya G, Reess T, Pécastaing L, Gibert A and Domens P 2006 *J. Phys.* D: *Appl. Phys.* **39** 5236

[11] Jones H M and Kunhardt E E 1995 *J. Appl. Phys.* **28** 178

[12] Martin T H, Guenther A H and Kristiansen M 1996 *J. C Martin on Pulsed Power* (New York: Plenum)

[13] Korobeinikov S M 1998 *Bubble Model of Ignition of the Impulse Electric Discharge in Liquids* (Ph.D. Thesis) Tomsk

[14] Kukhta V R and Lopatin V V 1999 *Proceedings of* 13*th International Conference on Dielectric Liquids (ICDL*99*)* (Nara, Japan) p. 20

[15] Golant V E, Zhilinskii A P and Sakharov I E 1980 *Fundamentals of Plasma Physics* (New York: Wiley)

[16] Cook J, Gleeson A M and Roberts R M 1997 *J. Acoust. Soc. Am.* **101** 1908

[17] Lu X P, Pan Y and Zhang H H 2002 *Acta Phys. Sin.* **51** 1768 (in Chinese)